



Ferromagnetism With High Curie Temperature of Cu Doped LiMgN New Dilute Magnetic Semiconductors

Junquan Deng, Wuqing Yang, Aiyuan Hu, Peng Yu, Yuting Cui, Shoubing Ding* and Zhimin Wu*

Chongqing Key Laboratory of Photoelectric Functional Materials, College of Physics and Electronic Engineering, Chongqing Normal University, Chongqing, China

OPEN ACCESS

Edited by:

Xiaotian Wang,
Southwest University, China

Reviewed by:

Xu Li,
Chengdu University of Information
Technology, China
Yongtian Wang,
North China Electric Power University,
China
Liu Jun,
Chongqing University of Posts and
Telecommunications, China

*Correspondence:

Shoubing Ding
shoubingding@cqnu.edu.cn
Zhimin Wu
zmmwu@cqnu.edu.cn

Specialty section:

This article was submitted to
Computational Materials Science,
a section of the journal
Frontiers in Materials

Received: 18 August 2020

Accepted: 28 September 2020

Published: 23 February 2021

Citation:

Deng J, Yang W, Hu A, Yu P, Cui Y,
Ding S and Wu Z (2021)
Ferromagnetism With High Curie
Temperature of Cu Doped LiMgN New
Dilute Magnetic Semiconductors.
Front. Mater. 7:595953.
doi: 10.3389/fmats.2020.595953

New diluted magnetic semiconductors represented by Li(Zn,Mn)As with decoupled charge and spin doping have received much attention due to their potential applications for spintronics. However, their low Curie temperature seriously restricts the wide application of these spintronic devices. In this work, the electronic structures, ferromagnetic properties, formation energy, and Curie temperature of Cu doped LiMgN and the corresponding Li deficient system are calculated by using the first principles method based on density functional theory, combined with Heisenberg model in the Mean-Field Approximation. We find that the Cu doped systems have high temperature ferromagnetism, and the highest Curie temperature is up to 573K, much higher than the room temperature. Li(Mg_{0.875}Cu_{0.125})N is a half metallic ferromagnet and its net magnetic moments are 2.0 μ_B . When Li is deficient, the half metallic ferromagnetism becomes stronger, the magnetic moments increase to 3.0 μ_B . The bonding and differential charge density indicate that the half metallic ferromagnetism can be mainly attributed to the strong hybridization between N 2p and doped Cu 3d orbitals. The results show that Cu doped LiMgN is a kind of ideal new dilute magnetic semiconductor that will benefit potential spintronics applications.

Keywords: Cu doped LiMgN, electronic structures, ferromagnetism, Curie temperature, first-principles

INTRODUCTION

In the modern information technology, the transmission and processing of information mainly use the charge of electrons, while the storage of information mainly uses the spin of electrons. The two degrees of freedom are independent of each other. Diluted magnetic semiconductors (DMS) utilize the electron's charge and spin degrees of freedom simultaneously to achieve novel quantum functionalities, which can combine the properties of semiconductor with ferromagnetism and have potential applications in spintronics (Ohno, 1998). Therefore, the designed spintronic devices have the advantages of lower energy consumption, faster running speed and smaller volume (Zutic et al., 2004; Dietl, 2010; Kacimi et al., 2014). However, there are some insurmountable difficulties for traditional III-V group based dilute magnetic semiconductors prepared by doping transition metals. For example, since the magnetic moments and carriers are provided by the same doped element, the binding effect of the spin and charge precludes the possibility of tuning electric and magnetic properties individually (Kaczowski and Jezierski, 2009). The heterovalent substitution of Mn²⁺ into Ga³⁺ leads to severely chemical solubility of the magnetic ions (Potashnik et al., 2001). The average solubility for Mn is less than 1%, and only metastable films can be formed, resulting in that it is

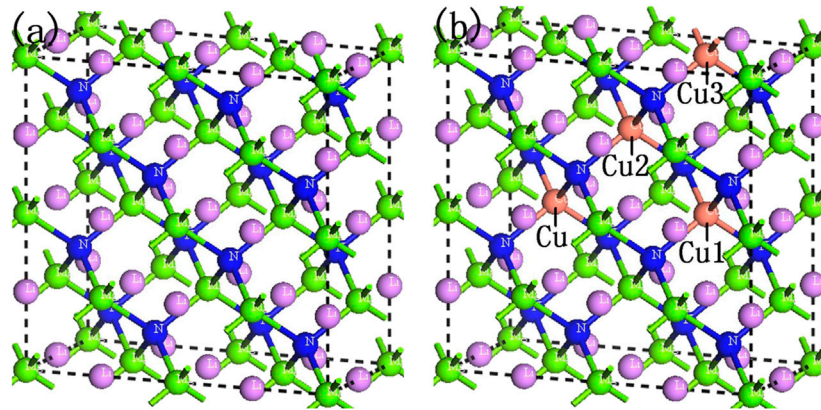


FIGURE 1 | Supercell structures of LiMgN with 48 atoms: **(A)** LiMgN, **(B)** Li(Mg_{0.875}Cu_{0.125})N.

difficult to study the origin and mechanism of magnetism in dilute magnetic semiconductors Potashnik et al., 2001). Besides, the impurity ions often have higher ionization energy, restricting the contribution of free carriers in the system (Yan et al., 2007).

To overcome these difficulties, Mašek et al. (2007) theoretically proposed a kind of new diluted magnetic semiconductor Li(Zn,Mn)As based on I-II-V group elements, wherein magnetism due to isovalent substitution can be decoupled from carrier doping with excess/deficient Li concentrations. Deng et al. (2011), Jin et al. (2013) successfully prepared polycrystalline Li(Zn,Mn)As bulk materials with T_C as high as ~ 50 K. Muon spin rotation measurements have established that the magnetically ordered volume reaches 100% below T_C , and the magnitudes of the ferromagnetic exchange coupling and the ordered moment are comparable to those of (Ga,Mn)As (Deng et al., 2011). Sato et al. (2012) theoretically calculated the electronic structures of Mn doped LiZnAs, LiZnP and LiZnN, and found that introduced Li vacancies could strongly suppress spinodal decomposition, induce ferromagnetic interaction and improve T_C in these systems. Following this, a series of new generation diluted ferromagnetic semiconductors, e.g., “111” type Li(Zn,Mn)P (Deng et al., 2013; Ding et al., 2013) and Li(Cd,Mn)P (Han et al., 2019), “122” type (Ba,K)(Zn,Mn)₂As₂ (Zhao et al., 2013; Zhao et al., 2014), “1111” type (La,Ca)(Zn,Mn)SbO (Ding et al., 2014), and “32522” type (Sr₃La₂O₅)(Zn,Mn)₂As₂ (Man et al., 2014), were successfully synthesized. A number of progresses of these new DMSs have been made on both fundamental studies and potential applications. Among them, the highest T_C is 230 K of the (Ba,K)(Zn,Mn)₂As₂ system (Zhao et al., 2014). However, it remains below room temperature.

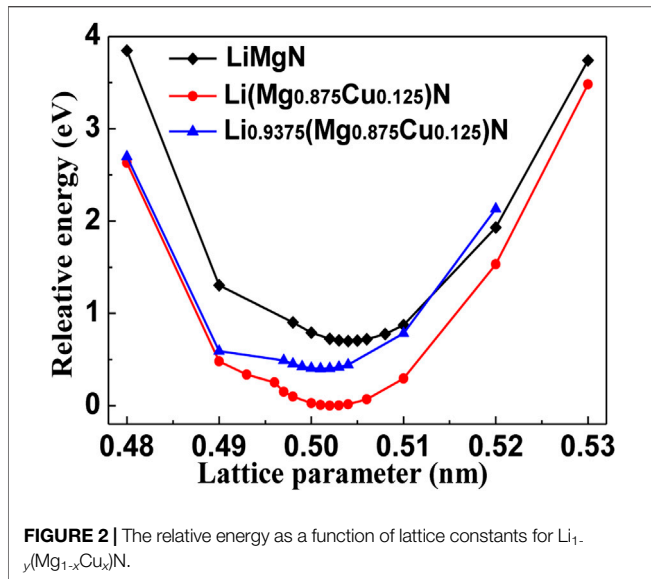
Improvement of T_C is always a fundamental issue for diluted ferromagnetic semiconductor materials. To explore new dilute magnetic semiconductor materials with better performance, in this work, the electronic structures, ferromagnetic properties, formation energy, and Curie temperature of Cu doped LiMgN and the corresponding Li deficient system are investigated by using the first principle calculation method based on density functional theory (DFT), combined with Heisenberg model in the

Mean-Field Approximation. We find that the Cu doped systems have high temperature ferromagnetism, the highest T_C is up to 573 K, which indicate that Cu doped LiMgN is a kind of ideal new dilute magnetic semiconductor.

COMPUTATIONAL DETAILS

LiMgN is an antifluorite structure (Kuriyama et al., 2002) with the lattice constant $a = b = c = 4.955$ Å, belongs to the space group $F-43m$. It can be prepared by the reaction of Li, Mg and N₂ at high temperature (800°C) (Kuriyama et al., 2002). The LiMgN tetrahedral lattice can be viewed as a zinc blende MgN binary compound, analogous to GaN, filled with Li atoms at tetrahedral interstitial sites near N. In the present work, a $2 \times 2 \times 1$ (48 atoms) supercell of ZB-type LiMgN was constructed, containing 16 Li, 16 Mg and 16 N atoms, as shown in **Figure 1A**. Two Mg atoms were substituted by two Cu atoms, thus the doping concentration was 12.5%. When one Cu atom was fixed, another Cu atom was selected three asymmetric positions for comparison (as shown in **Figure 1B**). One Li atom closest to the Cu atom was removed in order to introduce a Li vacancy (V_{Li}) in the $2 \times 2 \times 1$ supercell.

All the first-principles calculations were carried out with the Cambridge Serial Total Energy Package (CASTEP) code (Segall et al., 2002) based on the density functional theory (DFT) method. The periodic boundary conditions were applied in all calculations, and the generalized gradient approximation (GGA) in Perdew Burke Ernzerhof (PBE) (Perdew et al., 1996) was performed to deal with the electronic exchange-correlation potential energy. In order to reduce the number of the plane wave basis vectors groups, the plane-wave ultrasoft pseudo potential (USPP) method (Vanderbilt, 1990) was implemented to describe the interaction between ionic core and valence electrons. The valence electronic states were Li:2s¹, Mg:2p⁶3s², N:2s²2p³ and Cu:3d¹⁰4s¹, respectively. The cut-off energy for the plane-wave was 400 eV, and the Monkhorst-Pack mesh was $3 \times 3 \times 6$ for the integral calculation of the total energy and charge



density in the Brillouin zone. The self-consistent convergence accuracy was set at 2.0×10^{-6} eV/atom. The structures of each doped configuration were optimized before the calculations of total energies and the electronic structures.

RESULTS AND DISCUSSION

Electronic Structures

In order to achieve the equilibrium lattice constants, the structures of $\text{Li}_{1-y}(\text{Mg}_{1-x}\text{Cu}_x)\text{N}$ were optimized firstly. The geometry optimization curves are plotted in **Figure 2**. It can be seen that the optimized lattice constant for LiMgN is 5.04 Å, which is slightly overestimated comparing with the experimental value (4.955 Å) (Kuriyama et al., 2002). The optimized lattice constants of Li ($\text{Mg}_{0.875}\text{Cu}_{0.125}$) and $\text{Li}_{0.9375}(\text{Mg}_{0.875}\text{Cu}_{0.125})\text{N}$ are 5.02 and 5.01 Å respectively, slightly less than that of the pure LiMgN.

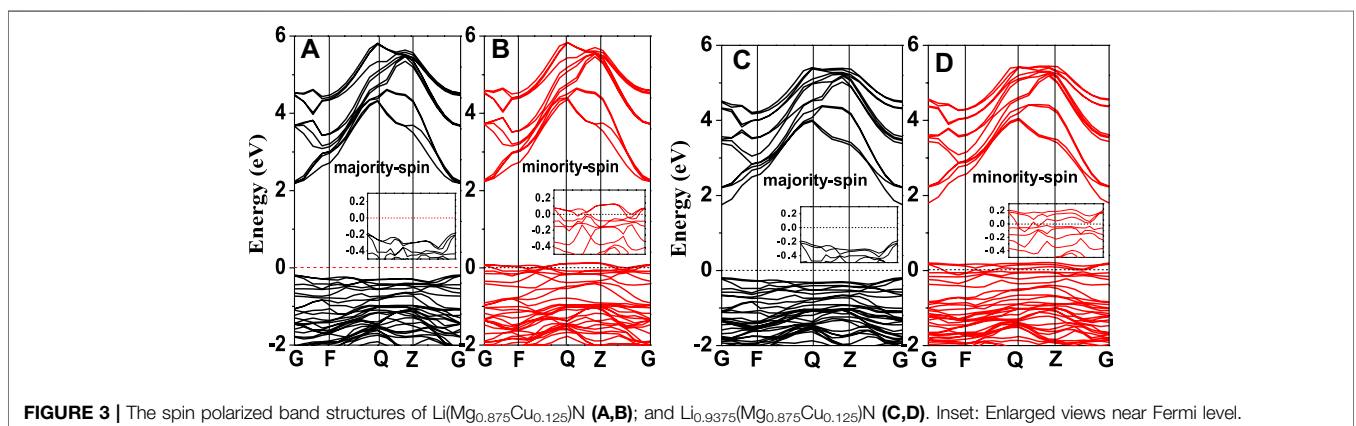
Pure LiMgN is a direct band gap semiconductor. The valence band is mainly composed of N-2p, Mg-2p state

TABLE 1 | The band gaps (E_g), the spin-flip/half-metallic gaps (HM gap), magnetic moments (M), and formation energies (E_f) of $\text{Li}_{1-y}(\text{Mg}_{0.875}\text{Cu}_{0.125})\text{N}$.

$\text{Li}_{1-y}(\text{Mg}_{1-x}\text{Cu}_x)\text{N}$	E_g (eV)	HM gap (eV)	M (μ_B)	E_f (eV)
$\text{Li}(\text{Mg}_{0.875}\text{Cu}_{0.125})\text{N}$	2.23	0.13	2.0	1.98
$\text{Li}_{0.9375}(\text{Mg}_{0.875}\text{Cu}_{0.125})\text{N}$	1.98	0.22	3.0	3.56

and Li-2s electronic states, and the conduction band is mainly composed of Mg-2p and Mg-3s electronic states. **Figure 3** shows the spin polarized energy band structures of Cu doped LiMgN and the corresponding Li deficient system, and the inset is enlarged views of the vicinity of Fermi level. It can be seen in **Figures 3A,B** that some impurity levels are introduced near the Fermi level by Cu doping. In the majority-spin bands, the impurity bands merge into the valence band top, and the Fermi level still lies in the band gap, so the majority-spin bands remain semiconducting nature. While in the minority-spin bands, the Fermi level penetrates through the impurity bands, resulting in that two of the impurity levels cross the Fermi level, which demonstrates that the minority-spin bands exhibit metallic properties. So the Cu doped LiMgN system becomes a half-metallic material with 100% spin-polarized ratio of conduction electron. The spin-flip band gap is 0.13 eV (shown in **Table 1**). **Figures 3C,D** are the energy band structures of Cu doped LiMgN with Li vacancies. They are similar to that of Cu doped LiMgN, indicates that $\text{Li}_{0.9375}(\text{Mg}_{0.875}\text{Cu}_{0.125})\text{N}$ also exhibits half metallic property. However, the minority-spin bands are somewhat different. The impurity levels across the Fermi level increase to three, and the spin-flip band gap increases to 0.22 eV, which indicates that the more robust half-metallic behavior to lattice deformation and temperature for Li deficient system.

Figure 4 shows the density of states (DOS) of Cu doped LiMgN and the corresponding Li deficient system. It can be seen in **Figure 4A** that the sub-bands crossing the Fermi level mainly come from Li-2s, N-2p and Cu-3d states of the minority-spin. Besides, one can also note that a resonance peak appears near the Fermi surface, indicating that the electron orbitals of Li-2s, N-2p and Cu-3d states have strong sp-d hybridization near the Fermi



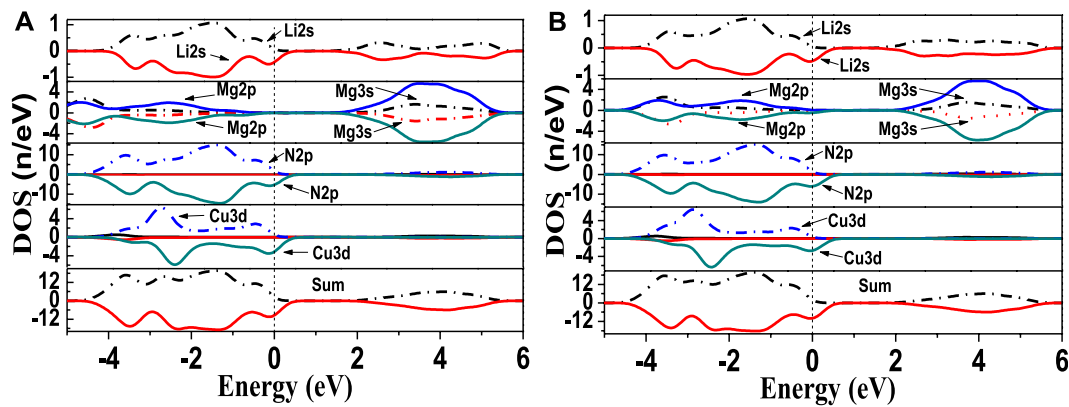


FIGURE 4 | The density of states of Li(Mg_{0.875}Cu_{0.125})N (A); Li_{0.9375}(Mg_{0.875}Cu_{0.125})N (B).

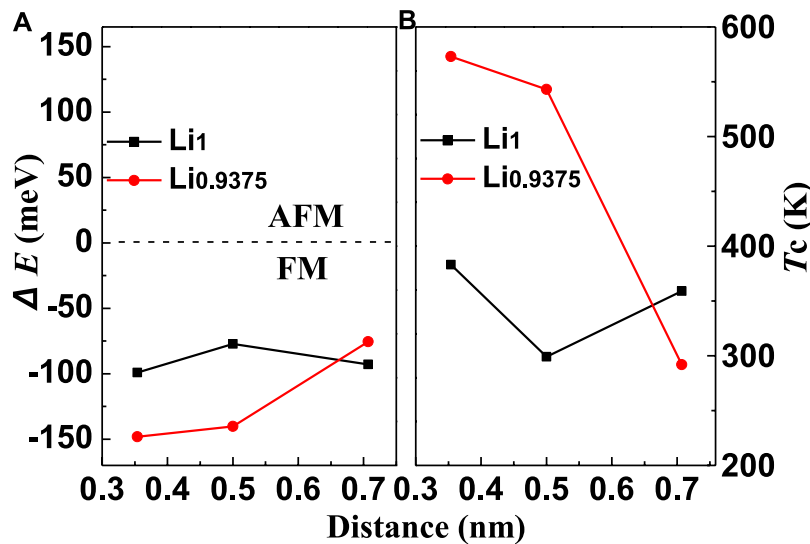


FIGURE 5 | The energy difference of the ferromagnetic and antiferromagnetic state (A) and the Curie temperature (B) as a function of the two doped Cu atoms distance for Li_{1-y}(Mg_{0.875}Cu_{0.125})N.

level. The t_{2g} energy level split from Cu-3d states of the minority-spin is pushed across the Fermi level, which makes it become a half-filled state. This causes that the states of the majority-spin are slightly more than those of the minority-spin, resulting in the net magnetic moments. The calculated net magnetic moments are $2.0 \mu_B$ for Li(Mg_{0.875}Cu_{0.125})N as shown in Table 1. Figure 4B shows that when Li is deficient, the DOS of Li-2s, N-2p and Cu-3d states near the Fermi level increase obviously. This indicates that the Li vacancies enhance the sp-d orbital hybridization. The t_{2g} energy levels are pushed further above the Fermi level, which makes none of the three levels is occupied by electrons. This increases the spin-flip band gap and net magnetic moments for Li_{0.9375}(Mg_{0.875}Cu_{0.125})N. The formation energy of the two systems is also calculated and shown in Table 1. The stability of the doped system decreases slightly with respect to pure LiMgN.

Ferromagnetism and Bonding

To explore the magnetic properties of the systems, the ferromagnetic and antiferromagnetic coupling energy of Li_{1-y}(Mg_{0.875}Cu_{0.125})N with different Cu doped position are calculated and shown in Table 2, where E_{FM} is the ferromagnetic coupling energy of the systems, E_{AFM} is the antiferromagnetic coupling energy, and ΔE is the difference between the ferromagnetic and antiferromagnetic coupling energy. It can be seen obviously that $\Delta E < 0$ for each doped position, indicating that the ferromagnetic order is more stable than the antiferromagnetic order. The Cu doped LiMgN systems are half-metallic ferromagnet. To further understand the ferromagnetic properties of Li_{1-y}(Mg_{0.875}Cu_{0.125})N, the variation of ΔE with the distance between two Cu atoms is plotted in Figure 5A. It can be seen that ΔE decreases with the distance, implying that the half-metallic ferromagnetism

TABLE 2 | The ferromagnetic and anti-ferromagnetic coupling energy of $\text{Li}_{1-y}(\text{Mg}_{0.875}\text{Cu}_{0.125})\text{N}$ with different Cu doped position.

$\text{Li}_{1-y}(\text{Mg}_{1-x}\text{Cu}_x)\text{N}$	Cu atoms distance (nm)	E_{FM} (eV)	E_{AFM} (eV)	$\Delta E = E_{\text{FM}} - E_{\text{AFM}}$ (meV)
$\text{Li}(\text{Mg}_{0.875}\text{Cu}_{0.125})\text{N}$ -1	0.500	-23988.64142	-23988.56416	-77.26
$\text{Li}(\text{Mg}_{0.875}\text{Cu}_{0.125})\text{N}$ -2	0.354	-23988.84502	-23988.74593	-99.09
$\text{Li}(\text{Mg}_{0.875}\text{Cu}_{0.125})\text{N}$ -3	0.707	-23988.67494	-23988.58214	-92.80
$\text{Li}_{0.9375}(\text{Mg}_{0.875}\text{Cu}_{0.125})\text{N}$ -1	0.500	-23796.27993	-23796.13969	-140.24
$\text{Li}_{0.9375}(\text{Mg}_{0.875}\text{Cu}_{0.125})\text{N}$ -2	0.354	-23796.48006	-23796.33201	-148.05
$\text{Li}_{0.9375}(\text{Mg}_{0.875}\text{Cu}_{0.125})\text{N}$ -3	0.707	-23796.38217	-23796.30667	-75.50

TABLE 3 | The charge population overlap and bond length of the chemical bonds for $\text{Li}_{1-y}(\text{Mg}_{1-x}\text{Cu}_x)\text{N}$.

$\text{Li}_{1-y}(\text{Mg}_{1-x}\text{Cu}_x)\text{N}$	Chemical bonds	Charge population overlap	Bond length (Å)
LiMgN	Li-N	-0.02	2.182
	Mg-N	-0.03	2.182
$\text{Li}(\text{Mg}_{0.875}\text{Cu}_{0.125})\text{N}$	Li-N	-0.11	2.173
	Mg-N	-0.08	2.173
	Cu-N	0.70	2.173
$\text{Li}_{0.9375}(\text{Mg}_{0.875}\text{Cu}_{0.125})\text{N}$	Li-N	-0.12	2.169
	Mg-N	-0.25	2.169
	Cu-N	0.71	2.169

become stronger as the two Cu atoms is closer. Moreover, when Li is deficient, the half-metallic ferromagnetism is further enhanced.

The ideal DMS should have Curie temperature (T_c) higher than the room temperature. The Curie temperature of the Cu doped LiMgN systems is estimated by using the Heisenberg model in the Mean-Field Approximation (Sato et al., 2003):

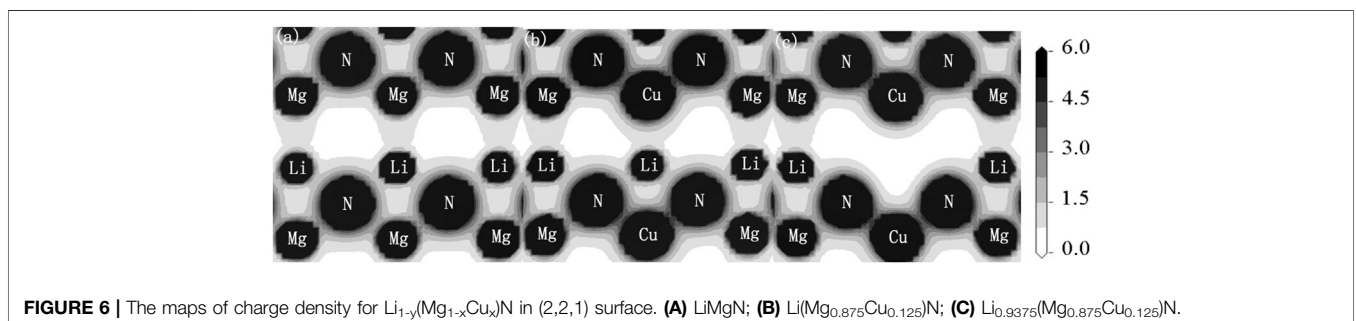
$$K_B \bullet T_c = 2\Delta E/3x \quad (1)$$

where x is the number of doped particles, ΔE is the difference between the ferromagnetic and antiferromagnetic coupling energy, and K_B is the Boltzmann constant. The variation of T_c with the distance between two Cu atoms is shown in **Figure 5B**. It can be seen that T_c of the doped systems is significantly enhanced when Li is deficient, and the maximum T_c is up to 573 K, much higher than the room temperature. Which shows that Cu doped LiMgN is a kind of ideal new dilute magnetic semiconductor that will benefit potential spintronics applications.

Table 3 shows the bond length and charge population overlap of the doped systems. It is found that the numbers of the charge population overlap for the Li-N and Mg-N bonds in pure LiMgN are negative, which indicates that they are ionic bonds. For Cu doped system, the numbers of the charge population overlap for Li-N and

Mg-N bonds decrease. Meanwhile, the number of the charge population overlap for Cu-N bond is positive, demonstrating the covalent nature for the Cu-N bond, which is due to the strong hybridization between N 2p and doped Cu 3d orbitals. In general, the radius of Cu ion is larger than that of Mg ion. However, the bond length decreases for Cu doped system because of the Cu-N covalent bond nature, resulting in that the lattice constant also decreases. When Li is deficient, the numbers of the charge population overlap for Li-N and Mg-N bonds further decreases, whereas that of Cu-N bond further increases. This indicates that more charges transfer from the Li and Mg atoms to the Cu and N atoms, resulting in that the covalent nature for the Cu-N bond become stronger.

Figure 6 shows the charge density for $\text{Li}_{1-y}(\text{Mg}_{1-x}\text{Cu}_x)\text{N}$ along (2,2,1) plane. It can be seen that the values of charge density around Li and Mg atoms (**Figure 6B**) also decrease compared with those of pure LiMgN (**Figure 6A**). Besides, we can find that the charges transfer from the Li and Mg atoms to the Cu and N atoms, resulting in that the interaction between Cu and N atoms is stronger than that between Mg and N atoms. When Li is deficient, the charges further transfers and the interaction between Cu and N atoms become stronger. These results indicate that the effect of Cu doping on the ferromagnetic properties and bonding of the doped system is mainly

**FIGURE 6** | The maps of charge density for $\text{Li}_{1-y}(\text{Mg}_{1-x}\text{Cu}_x)\text{N}$ in (2,2,1) surface. (A) LiMgN; (B) $\text{Li}(\text{Mg}_{0.875}\text{Cu}_{0.125})\text{N}$; (C) $\text{Li}_{0.9375}(\text{Mg}_{0.875}\text{Cu}_{0.125})\text{N}$.

attributed to the strong hybridization between N 2p and doped Cu 3d orbitals.

CONCLUSION

In this work, the electronic structures, ferromagnetism, formation energy, and Curie temperature of Cu doped LiMgN and the corresponding Li deficient system are calculated by using the first principles method based on density functional theory, combined with Heisenberg model in the Mean-Field Approximation. We find that the Cu doped systems exhibit half-metallic ferromagnetism, which is helpful for spin injection. The net magnetic moments for $\text{Li}(\text{Mg}_{0.875}\text{Cu}_{0.125})\text{N}$ are $2.0 \mu_B$. When Li is deficient, the half-metallic ferromagnetism becomes stronger, the magnetic moments increase to $3.0 \mu_B$. The density of states, bonding and charge density indicate that the half-metallic ferromagnetism can be mainly attributed to the strong hybridization between N 2p and doped Cu 3d orbitals. Besides, we also find that the highest Curie temperature is up to 573 K when Li is deficient, much higher than the room temperature. These results indicate that Cu doped LiMgN is a

kind of ideal new dilute magnetic semiconductor and will benefit potential spintronics applications.

DATA AVAILABILITY STATEMENT

All datasets presented in this study are included in the article/Supplementary Material.

AUTHOR CONTRIBUTIONS

All authors listed have made a substantial, direct, and intellectual contribution to the work and approved it for publication.

FUNDING

The work described in this paper is supported by Chongqing Natural Science Foundation of China (Grant No. cstc2019jcyj-msxmX0251).

REFERENCES

- Deng, Z., Jin, C. Q., Liu, Q. Q., Wang, X. C., Zhu, J. L., Feng, S. M., et al. (2011). $\text{Li}(\text{Zn},\text{Mn})\text{As}$ as a new generation ferromagnet based on a I-II-V semiconductor. *Nat. Commun.* 2, 422. doi:10.1038/ncomms1425
- Deng, Z., Zhao, K., Gu, B., Han, W., Zhu, J. L., Wang, X. C., et al. (2013). Diluted ferromagnetic semiconductor $\text{Li}(\text{Zn},\text{Mn})\text{P}$ with decoupled charge and spin doping. *Phys. Rev. B* 88, 081203. doi:10.1103/PhysRevB.88.081203
- Dietl, T. (2010). A ten-year perspective on dilute magnetic semiconductors and oxides. *Nat. Mater.* 9, 965. doi:10.1038/nmat2898
- Ding, C., Gong, X., Man, H., Zhi, G., Guo, S., Zhao, Y., et al. (2014). The suppression of curie temperature by Sr doping in diluted ferromagnetic semiconductor $(\text{La}_{1-x}\text{Sr}_x)(\text{Zn}_{1-y}\text{Mn}_y)\text{AsO}$. *Eur. Phys. Lett.* 107, 17004. doi:10.1209/0295-5075/107/17004
- Ding, C., Qin, C., Man, H. Y., Imai, T., and Ning, F. L. (2013). NMR investigation of the diluted magnetic semiconductor $\text{Li}(\text{Zn}_{1-x}\text{Mn}_x)\text{P}$ ($x = 0.1$). *Phys. Rev. B* 88, 041108. doi:10.1103/PhysRevB.88.041102
- Han, W., Chen, B. J., Gu, B., Zhao, G. Q., Yu, S., Wang, X. C., et al. (2019). $\text{Li}(\text{Cd},\text{Mn})\text{P}$: a new cadmium based diluted ferromagnetic semiconductor with independent spin & charge doping. *Sci. Rep.* 9, 7490. doi:10.1038/s41598-019-43754-x
- Jin, C. Q., Wang, X. C., Liu, Q. Q., Sijia, Z., ShaoMin, F., Zheng, D., et al. (2013). New quantum matters: build up versus high pressure tuning. *Sci. China Phys. Mech. Astron.* 56, 2337. doi:10.1007/s11433-013-5356-2
- Kacimi, S., Mehnan, H., and Zaoui, A. (2014). I-II-V and I-III-IV half-Heusler compounds for optoelectronic applications: comparative ab initio study. *J. Alloy. Compd.* 587, 451. doi:10.1016/j.jallcom.2013.10.046
- Kaczkowski, J., and Jezierski, A. (2009). Ab initio calculations of magnetic properties of wurtzite $\text{Al}_{0.9375}\text{TM}_{0.0625}\text{N}$ (TM = V, Cr, Mn, Fe, Co, Ni). *Acta Phys. Pol. A* 115, 275. doi:10.12693/APhysPolA.115.275
- Kuriyama, K., Nagasawa, K., and Kushida, K. (2002). Growth and band gap of the filled tetrahedral semiconductor LiMgN . *J. Cryst. Growth.* 237, 2019–2022. doi:10.1016/S0022-0248(01)02249-7
- Man, H., Qin, C., Ding, C., Wang, Q., Gong, X., Guo, S., et al. (2014). $(\text{Sr}_3\text{La}_2\text{O}_5)(\text{Zn}_{1-x}\text{Mn}_x)_2\text{As}_2$: a bulk form diluted magnetic semiconductor isostructural to the “32522” Fe-based superconductors. *Eur. Phys. Lett.* 105, 67004. doi:10.1209/0295-5075/105/67004
- Mašek, J., Kudrnovský, J., Máca, F., Gallagher, B. L., Campion, R. P., Gregory, D. H., et al. (2007). Dilute moment n-type ferromagnetic semiconductor $\text{Li}(\text{Zn},\text{Mn})\text{As}$. *Phys. Rev. Lett.* 98, 067202. doi:10.1103/PhysRevLett.98.067202
- Ohno, H. (1998). Making nonmagnetic semiconductors ferromagnetic. *Science* 281, 951. doi:10.1126/science.281.5379.951
- Perdew, J. P., Burke, K., and Ernzerhof, M. (1996). Generalized gradient approximation made simple. *Phys. Rev. Lett.* 77, 3865. doi:10.1103/PhysRevLett.77.3865
- Potashnik, S. J., Ku, K. C., Chun, S. H., Berry, J. J., Samarth, N., and Schiffer, P., (2001). Effects of annealing time on defect-controlled ferromagnetism in $\text{Ga}_{1-x}\text{Mn}_x\text{As}$. *Appl. Phys. Lett.* 79, 1495. doi:10.1063/1.1398619
- Sato, K., Dederichs, P. H., and Katayama-Yoshida, H. (2003). Curie temperatures of III-V diluted magnetic semiconductors calculated from first principles. *Europhys. Lett.* 61, 403. doi:10.1209/epl/2003-00191-8
- Sato, K., Fujimoto, S., Fujii, H., Fukushima, T., and Katayama-Yoshida, H., (2012). Computational materials design of filled tetrahedral compound magnetic semiconductors. *Physica B* 407, 2950. doi:10.1016/j.physb.2011.09.036
- Segall, M. D., Lindan, P. J. D., Probert, M. J., Pickard, C. J., Hasnip, P. J., Clark, S. J., et al. (2002). First-principles simulation: ideas, illustrations and the CASTEP code. *J. Phys. Condens. Matter* 14, 2717. doi:10.1088/0953-8984/14/11/301
- Vanderbilt, D. (1990). Soft self-consistent pseudopotentials in a generalized eigenvalue formalism. *Phys. Rev. B Condens Matter* 41, 7892. doi:10.1103/physrevb.41.7892
- Yan, Y., Li, J., Wei, S. H., and Al-Jassim, M. M. (2007). Possible approach to overcome the doping asymmetry in wideband gap semiconductors. *Phys. Rev. Lett.* 98, 135506. doi:10.1103/PhysRevLett.98.135506
- Zhao, K., Deng, Z., Wang, X. C., Han, W., Zhu, J. L., Li, X., et al. (2013). New diluted ferromagnetic semiconductor with Curie temperature up to 180 K and isostructural to the ‘122’ iron-based superconductors. *Nat. Commun.* 4, 1442. doi:10.1038/ncomms2447
- Zhao, K., Chen, B. J., Zhao, G. Q., Yuan, Z., Liu, Q., Deng, D., et al. (2014). Ferromagnetism at 230 K in $(\text{Ba}_{0.7}\text{K}_{0.3})(\text{Zn}_{0.85}\text{Mn}_{0.15})_2\text{As}_2$ diluted magnetic semiconductor. *Chin. Sci. Bull.* 59, 2524. doi:10.1007/s11434-014-0398-z
- Zutic, I., Fabian, J., and Das Sarma, S. (2004). Spintronics: fundamentals and applications. *Rev. Mod. Phys.* 76, 323. doi:10.1103/RevModPhys.76.323

Conflict of Interest: The authors declare that the research was conducted in the absence of any commercial or financial relationships that could be construed as a potential conflict of interest.

Copyright © 2021 Deng, Yang, Hu, Yu, Cui, Ding and Wu. This is an open-access article distributed under the terms of the Creative Commons Attribution License (CC BY). The use, distribution or reproduction in other forums is permitted, provided the original author(s) and the copyright owner(s) are credited and that the original publication in this journal is cited, in accordance with accepted academic practice. No use, distribution or reproduction is permitted which does not comply with these terms.